MULTIFRACTAL AND MONOFRACTAL SCALING IN A LABORATORY MAGNETOHYDRODYNAMIC TURBULENCE EXPERIMENT

D. A. SCHAFFNER[1] AND M. R. BROWN
Swarthmore College, Swarthmore, PA, USA; dschaffner@gmail.com

ABSTRACT

Both multifractal and monofractal scaling of structure function exponents are observed in the turbulent magnetic fluctuations of the Swarthmore Spheromak Experiment plasma. Structure function and probability distribution function (PDF) analysis exhibits multifractal scaling exponents in low frequency, inertial range fluctuations of the turbulence but monofractal scaling in higher frequency, dissipation range fluctuations. The transition from multifractal to monofractal scaling occurs rapidly suggesting a dissipation mechanism that is insensitive to turbulent structure scale size. Structure functions and PDFs are presented for both temporal and spatial measurements. Variations in the magnetic helicity in the plasma are also shown to modify multifractal scaling characteristics of the inertial range, but do not affect the monofractal scaling of the dissipation range.

Key words: methods: statistical – magnetohydrodynamics (MHD) – plasmas – turbulence

1. INTRODUCTION

This paper presents the results of a thorough intermittency analysis of the fluctuating magnetic fields in the Swarthmore Spheromak Experiment (SSX) plasma through the use of structure functions and probability distribution functions (PDFs) of increments of both temporal and spatial measurements. The primary observation from this analysis is that temporal regions of the magnetic fluctuation data that are shown to be consistent with dissipation range turbulence (Schaffner et al. 2014a) exhibit a structure function scaling that indicates self-similar structure, whereas temporal regions consistent with inertial range turbulence do not exhibit this self-similarity. These results are discussed in the context of the multifractal versus the monofractal structure function scaling behavior of turbulence (Paladin & Vulpiani 1987; Frisch 1995; Marsch & Tu 1997), where a lack of self-similarity can be attributed to the multifractal behavior of the system. Similar distinctions between the inertial range and the dissipation range scaling were made in recent solar wind observations (Kiyani et al. 2013), suggesting that physical mechanisms underlying the scaling in each regime may be universal between solar wind and laboratory-based MHD turbulence. Furthermore, the relatively fast transition from multifractal to monofractal scaling suggests a dissipation mechanism that may have an absolute scale, such as the generation of current sheets at the ion inertial scale length (Kiyani et al. 2009, 2010), and not one that is relative to the scale size of structures in the inertial range such as that observed in conventional fluid turbulence (Chevillard et al. 2005).

Trends in scaling with magnetic helicity injection are also explored. Previous work (Schaffner et al. 2014c) demonstrated that increased injected helicity in the SSX plasma system resulted in an increased intermittency of the raw $dB(t)/dt$ signal. Results reported here show that $B(t)$ formed from time integration of the raw $dB(t)/dt$ signal exhibits this same trend. The scaling behavior of the structure functions differ with helicity depending on whether they are constructed from data in the dissipation versus the inertial range. Inertial range scaling appears to vary more widely with helicity than the dissipation range. This indicates that variation of helicity injection has an effect only on intermittent structures generated in the inertial range, or on the physical mechanism, which does the generating. Conversely, the mechanism that governs intermittency in the dissipation range is not strongly affected by the overall helicity content of the plasma.

A structure function analysis has typically been utilized to extend spectral or correlation analyses of turbulent fluctuations to higher-order statistics, particularly in scenarios where Gaussian and self-similar properties appear to break down. Examined first in hydrodynamics (Anselmet et al. 1984; Frisch 1995), the use of the technique has been expanded to MHD fluids including the solar wind velocity fluctuations (Burlaga 1991), solar wind magnetic fluctuations (Burlaga 1992; Tu & Marsch 1995), and magnetospheric plasmas (Consolini et al. 1996; Hnat et al. 2003). The work has led to the development of models that attempt to reconcile the observation of intermittency and non-self-similar statistics in turbulence fluctuations with the 1941 Kolmogorov turbulence model, which implies a self-similar fluctuation structure and can be described in terms of a monofractal scaling exponent (Kolmogorov 1941; Frisch 1995). Such multifractal models relax global scale invariance to a local scale invariance. Physically, these models describe modifications of how energy is distributed to smaller scales from larger scales either through differences in the space-filling nature of the turbulence, such as the random β-model (Benzi et al. 1984) or through variations in the energy transfer rate from larger to smaller scales such as the log-normal model (Kolmogorov 1962), the p-model (Meneveau & Sreenivasan 1987), and the She–Leveque model (Dubrulle 1994; She & Leveque 1994). Multifractal scaling models can make predictions for dissipation scaling, in particular, addressing a reduction in scaling exponents by viscosity (Frisch & Vergassola 1991; Chevillard et al. 2005). Since these models were developed with isotropic and homogeneous turbulence of conventional neutral fluids, extending intermittency models to MHD turbulence has added complications. MHD turbulence is inherently anisotropic—due to the symmetry breaking caused by embedded magnetic fields —in addition to having fluctuations, energy transfer and

---

[1] Current affiliation: Bryn Mawr College, Bryn Mawr, PA, USA; dschaffner@brynmawr.edu

dissipation channels for both magnetic and velocity fields. While hydrodynamic intermittency models have been directly applied to MHD turbulence (Burlaga 1991; Pagel & Balogh 2002), modified models pertaining explicitly to MHD have also been developed (Carbone 1993; Biskamp 1994; Biskamp & Müller 2000; Müller & Biskamp 2000; Bol-dyrev 2002; Cho et al. 2003). Structure function analysis can be of particular use for extracting signatures of dissipation in MHD turbulence (Cho et al. 2003; Alexandrova et al. 2008; Kiyani et al. 2009, 2013).

2. EXPERIMENT

MHD turbulent fluctuations are produced inside the compact wind tunnel configuration of the SSX using a plasma gun source inside a flux-conserving copper boundary. A turbulent cascade is generated by the injection of large-scale (size of the column radius) magnetic structures by the gun, which evolve and relax under the constraint of constant magnetic helicity inside the flux-conserving column, transferring energy to smaller scales (Schaffner et al. 2014a). The copper cylinder is 15.5 cm in diameter and 86 cm long and situated inside a highly evacuated chamber ($\approx 1 \times 10^{-8}$ Torr). The details of the gun source and production of magnetic fluctuations have been previously reported (Brown & Schaffner 2014, 2015; Schaffner et al. 2014a). The gun produces a 120 μs discharge of plasma; though the plasma is pulsed, there is a window of time in which the energy input from the gun roughly balances the energy loss in the system, generating a period of stationarity of fluctuations (Brown & Schaffner 2014, 2015; Schaffner et al. 2014b). This time range, from 40 to 60 μs after initiation of the discharge, is extracted from each shot to form an ensemble for analysis. The diagnostic analyzed in this paper is of magnetic fluctuations using an array of 16 magnetic pickup channels. Each channel consists of a single-loop of magnetic wire, 3 mm in diameter. Three loops are oriented in each cylindrical coordinate direction (B_r, B_θ, B_z) and each triplet is separated by 0.46 cm spanning from about 1 cm off the cylindrical axis to the edge of the cylinder boundary. The injected helicity of the plasma is scanned from 0 to 7×10^{-5} Wb^2 which corresponds to a scan of the amount of flux provided to the gun core—from 0 to 1.5 mWb (Schaffner et al. 2014c).

3. ANALYSIS TECHNIQUES

The structure functions and PDFs are constructed by taking differences or increments at varying temporal or spatial separations. In this analysis, the increments of magnetic measurements are constructed in three ways; first, the increments of each orthogonal magnetic component (ΔB_r, ΔB_θ, and ΔB_z) are examined separately. Then, vector magnitude is created from the vector sum of the three components at each time step and differences between the magnitudes ($\Delta |B|$) at each time step are used for the analysis. Lastly, the magnitude of the vector difference between time points is used as the increment ($|\Delta B|$). The increments can be in terms of a spatial division or a temporal division. In the context of this experiment, the spatial increments are in units of separation distance between probe locations ($\Delta r_{\min} = 0.46$ cm) , while the temporal increments are in units of sampling cadence ($\Delta \tau_{\min} = 15.4$ ns), which corresponds to the sampling frequency of 65 MHz. Increments are then increased in

multiples of these minimum values. Maximum separation values are limited by physical distance or data acquisition time span, as well as the ability to generate enough statistics for a valid calculation, though the main focus of results here will be on scales much smaller than the available time span to avoid issues of non-stationarity.

For a given increment, Δx, the PDF of increments is constructed by computing and histogramming a list of ΔB's,

$$\Delta B = |B(x + \Delta x) - B(x)| \tag{1}$$

which can then be normalized to the standard deviation and the total number of increments available in the data set for each given Δx.

A PDF can describe the nature of the data in terms of its relative distribution with respect to a Gaussian distribution. Large excursions of values in the tail values of the distribution are then indicative of intermittent behavior in the time series signal—i.e., large jumps in values outside of the standard deviation of the mean. Physically, these excursions can be identified with mechanisms in the plasma such as current sheets or shocks.

Further insight into the physical nature of the plasma can be gained by comparing these PDFs over a range of scales. This can be accomplished qualitatively by examining how the PDFs themselves change, but can also be quantitatively accomplished by calculating moments of these distributions: these are the structure functions. The structure function can be constructed for a given Δx by computing the average of the increments raised to some order, p, as in,

$$S^p(\Delta x) = \langle |B(x_j + \Delta x) - B(x_j)|^p \rangle \tag{2}$$

again where j indicates the available increments to be summed over.

Analysis of structure functions can illuminate characteristics of the fluctuations, particularly when modeled as a power-law function,

$$S^p(\Delta x) = (\Delta x)^\zeta. \tag{3}$$

When plotted logarithmically, ζ is the slope of the structure function; this slope can indicate the relative level of intermittency compared between two signals. That is, the steeper the slope, the more intermittent (i.e., the larger the "fat tails") the signal is. A flat line is the extreme case and indicates a lack of intermittency in the signal. As one would expect, the structure function of a time series generated from a normal distribution has a flat structure function. Changes in slope with scale indicates a change in intermittency as a function of scale. It should be noted, however, that this trend is not a perfect predictor of the presence of intermittency. For example, it can be shown that a time series of fractional Brownian motion (fBm) can be constructed with the same structure function slope (Hnat et al. 2003), but fBm produces a Gaussian probability distribution of increments. However, when inter-mittency is known to be present based on the PDF of increments (as is true for this SSX data set) then the relationship between slope and degree of intermittency generally holds true.

If ζ scales as a linear function of order p (i.e., $\zeta(p) = Hp$), the system exhibits self-similarity at different scales. In this
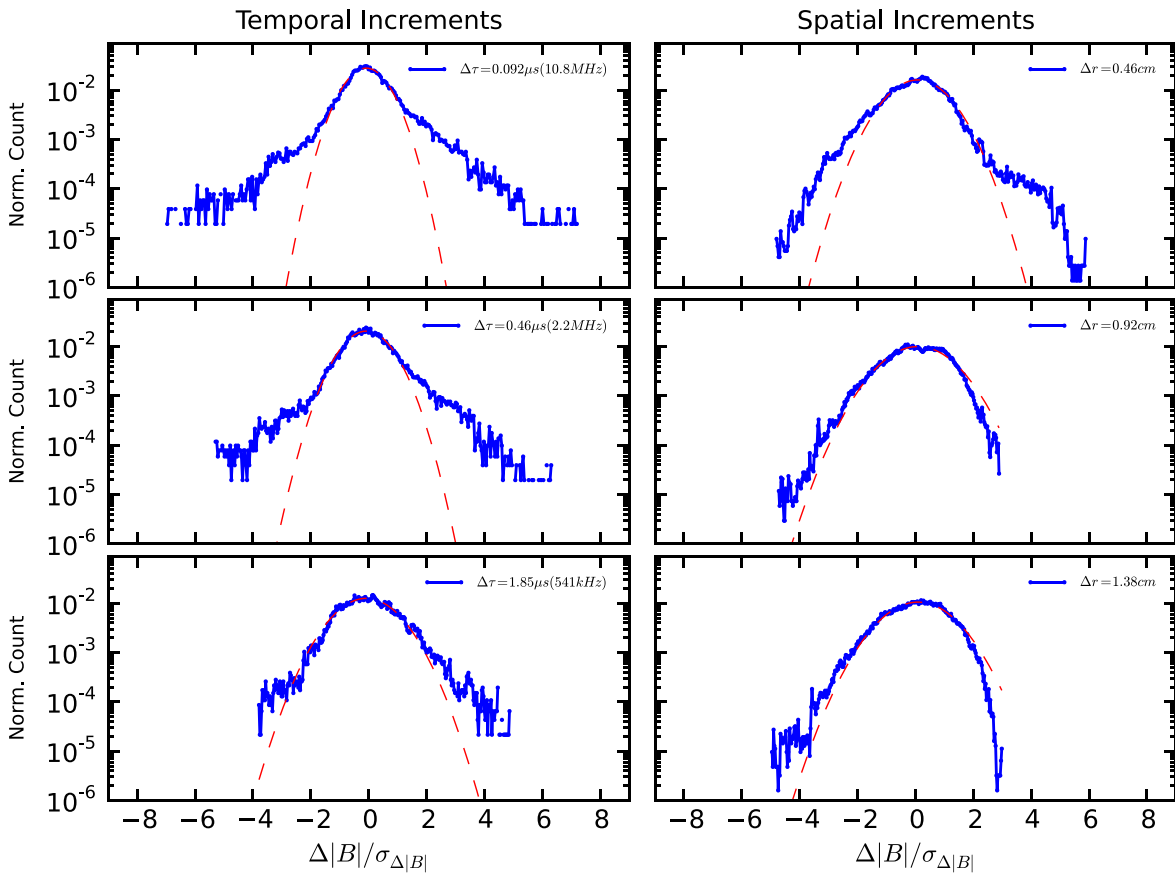
Figure 1. Probability distribution functions (PDFs) of increments for (a)–(c) temporal and (d)–(f) spatial measurements of $\Delta|B|$. The temporal increments are (a) 0.092 μs, (b) 0.46 μs, and (c) 1.85 μs while the spatial increments are (d) 0.46 cm, (e) 0.92 cm, and (f) 1.38 cm. Both temporal and spatial PDFs exhibit non-Gaussian tails indicating intermittency (Gaussian distributions are indicated with dashed red lines), but also that the level of intermittency decreases with increasing increment. Spatial PDFs appear to be slightly more asymmetric, which may be a result of boundary effects or low resolution compared to temporal measurements.

context, the self-similarity is a qualitative measure of how alike fluctuations appear at different scales. For example, a fractal from chaos theory is a construct that exhibits self-similarity. In other words, a self-similar system can be described in terms of a single fractal scaling or monofractal scaling description. The constant coefficient, H, is called the Hurst exponent; it can be shown that distributions that exhibit this self-similarity can be rescaled using the Hurst exponent as

$$\mathrm{PDF}\big(\Delta B, \Delta x^{-H}\big) = (\Delta x)^H \mathrm{PDF}(\Delta B, \Delta x). \qquad (4)$$

A nonlinear $\zeta(p)$, however, indicates non-self-similar behavior, exhibiting multiple fractal scalings simultaneously (i.e., multi-fractal behavior). These distinctions again can be used to elucidate possible physical mechanisms at play in the plasma.

In particular, it has been shown that differences in self-similarity exist between inertial range and dissipation range data in the solar wind (Kiyani et al. 2009, 2013). The slope of the structure functions of the solar wind inertial range were not linear as a function of order, indicating that these inertial range turbulent fluctuations do not exhibit self-similarity of turbulent structure and can be considered multifractal. On the other hand, the same analysis for dissipation range structure functions exhibited linear scaling—evidently, the physical mechanism behind the dissipation in the solar wind has a self-similar, scale-invariant nature—that is, monofractal behavior.

4. TEMPORAL AND SPATIAL PDFS OF INCREMENTS

Representative PDFs of both temporal and spatial magnetic field magnitude ($\Delta|B|$) increments are shown in Figure 1 with temporal PDFs on the left and spatial PDFs on the right. Each of the PDFs is scaled to its own standard deviation and total count so that they can be cross compared. The increments chosen for the temporal PDFs are 0.092 μs, 0.46 μs, and 1.85 μs which correspond to frequencies of 10.8 MHz, 2.2 MHz, and 541 kHz respectively. These three times also approximately correspond to three different regimes of the frequency spectra, called for lack of more accurate descriptions the dissipation, transition, and inertial regions. All three PDFs exhibit intermittent behavior as indicated by the wings or "fat tails" for large fluctuation values that reflect larger counts compared to a true Gaussian distribution, which is indicated by the dashed red curves in each subplot. Note, though, that the qualitative "level" of intermittency decreases with increasing temporal increment, consistent with previous intermittency analyses on SSX (Schaffner et al. 2014b, 2014c), as well as solar wind results (Bruno & Carbone 2013).

The increments chosen for the spatial PDFs are 0.46 cm, 0.92 cm, and 1.38 cm, which corresponds to the minimum, double the minimum, and triple the minimum separation possible given the probe array in the SSX. Unlike the temporal data, the spatial data is not believed to probe as far into dissipation range scales (for reference, an ion inertial length of 0.6 cm and an ion gyroradius of 0.1 cm are calculated for this
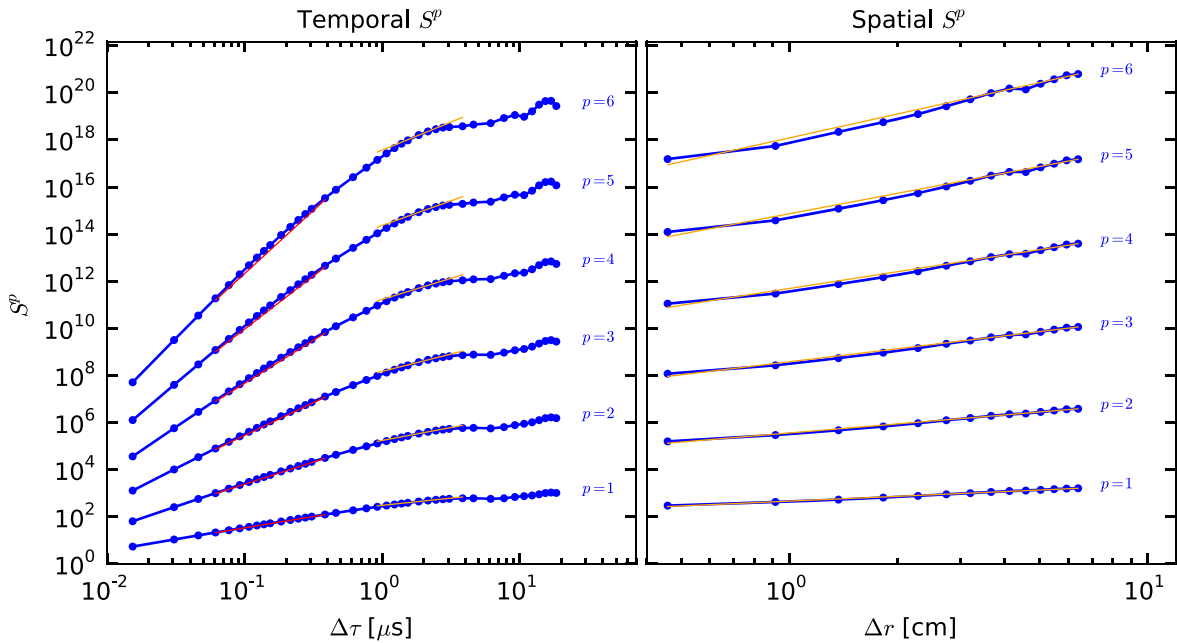
Figure 2. Structure functions of temporal (left) and spatial (right) measurements for integer orders $p = 1$ to $p = 6$. Fits to regions of the temporal structure functions are made to compute scaling exponents, ζ; separate regions are selected based on the breakdown of the frequency spectrum shown in Schaffner et al. (2014a) which occurs at approximatly 1 MHz or 1 μs. Spatial measurements likely span only the inertial range and thus only one region is fit.

plasma). Thus the spatial data is likely representative of inertial range turbulence and at most transition range. The resulting PDFs support this notion as they tend to have a more Gaussian-like distribution for small fluctuations and only slightly elevated tails. There does appear to be a trend toward increasing Gaussian-ness with an increasing increment similar to the temporal data. However, the curves do not appear as smooth as the temporal data because the histograms have larger breaks—in particular, the 0.46 cm increment PDF. This potentially reflects both a lower amount of increment statistics available for the spatial measurement as well as effects due to spatial variation of the plasma. Asymmetry of the spatial PDFs can also be seen; however, this is likely due to influences of the boundary of which the temporal data is much less susceptible. Finer resolution of the spatial measurements would also likely improve the symmetry of the PDFs in addition to allowing observation of the dissipation scale; such improved measure-ments are currently being attempted.

As discussed before, the use of PDFs of increments can clearly demonstrate the lack or presence of intermittent behavior in a signal, however, in a primarily qualitative way. Structure function analysis is needed to unearth the fractal scaling nature of the turbulence.

5. STRUCTURE FUNCTIONS AND SCALING WITH ORDER

To produce a more quantitative metric from the PDFs of increments, one can calculate moments of the histogram to any order p, and for each time or spatial delay Δx. This is equivalent to calculating the structure function in Equation (2) for the magnetic field increments. Integer values of p correspond to the moments of the PDF ($p = 2$ is the second moment, $p = 3$ is the third moment, etc.) though given the form of Equation (2), p is not restricted to integer values in the structure function formalism.

Figure 2 shows the structure functions, $S^p(\Delta x)$, for temporal ($\Delta x = \Delta\tau$) data on the left and spatial ($\Delta x = \Delta r$) data on the right. The integer structure functions from $p = 1$ to $p = 6$ are shown. The structure functions vary as a function of τ or r, which confirms the presence of intermittency in the signal. For the temporal results, it is clear that this variation changes as a function of timescale, with steeper slopes at small values of τ transitioning to shallower slopes at large values of τ. This indicates that the relative degree of intermittency of the signal increases when analyzed at smaller scales. The scale where the slope changes is consistent with the transition from the inertial to the dissipation range of the cascade as determined by the change in spectral index of the frequency spectrum for this plasma (Schaffner et al. 2014a). This difference between inertial and dissipation range intermittency suggests that the physical mechanism underlying the dissipation dynamics has a stronger intermittent nature. Explanations for this behavior in the solar wind typically focus on the presence of current sheets in the magnetic turbulence (Osman et al. 2014). The observation of this difference between dissipation and inertial range fluctuations in this laboratory plasma also suggests the existence of current sheets (Schaffner et al. 2014c).

The spatial structure functions do not show a change in slope with scale; the magnitude of the slope, and thus the degree of intermittency, is consistent with the temporal structure func-tions in the inertial range. Since the spatial measurements can only probe inertial range scales in the plasma, this result supports the distinction between dissipation and inertial range intermittency seen in the temporal data.

It can also be instructive to normalize the structure functions and, in particular, highlight the "level" of non-Gaussianness of a distribution. A normalized structure function can be constructed as

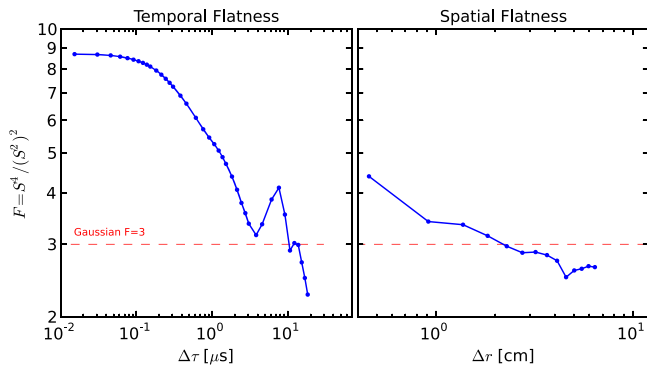$$S^p_{\text{norm}}(\Delta x) = \frac{S^p(\Delta x)}{\left(S^2(\Delta x)\right)^{(p/2)}} \qquad (5)$$

Figure 3. Normalized fourth order structure functions (a.k.a flatness or kurtosis) for temporal (left) and spatial (right) measurements. The flatness of a Gaussian signal is indicated by the dashed line at $F = 3$. Both figures show increasing flatness with decreasing scale, indicating a rise in intermittency.

where p is the order of the moment. Using this normalized structure function, a Gaussian time series would have a constant value. For example, for $p = 4$, this quantity becomes the flatness or kurtosis. Figure 3 shows the flatness for both temporal and spatial data. A Gaussian timeseries would have a constant value of three. Both Figure 3(a) and (b) show an excursion from a Gaussian distribution at smaller increments, though it is clearly more pronounced for the temporal data.

The self-similarity or fractal behavior of the turbulence, can be extracted from the structure function analysis by examining the slope of the structure functions as a function of order. The red lines in Figure 2 are fits to the structure functions. In the temporal data, fits are applied to two separate regions that correspond to the dissipation and inertial regions based on spectral frequency analysis, while the spatial data has only one fit for the entire region. A fit is made in each of these regions for each structure function using order p which ranges between 0.1 and 10 in steps of 0.1. The results of this scan are displayed in Figure 4 for both time and space. The five separate magnetic field measurements are shown now, with inertial range fits indicated by solid lines and dissipation range fits indicated with dashed lines. In this construction, a time series that exhibits self-similarity or monofracticality would produce a line with a constant slope. As the increments are raised to increasingly higher powers, the value of the structure function should also increase power-law-like. If the signal is self-similar, an increment between two points in the time series at one scale should have, on average, the same relative increment between two points at a different scale. In other words, a big fluctuation compared to a small fluctuation at one scale should appear to have the same relative ratio at a different scale. Thus, the structure function should change at a constant rate based on this ratio. If the signal is not self-similar, then the ratio is not constant and differences are increasingly accentuated by the raised exponent resulting in a nonlinear scaling.

Since the original Kolmogorov turbulence theory (Kolmogorov 1941) assumes a self-similar scaling, it predicts that the structure function slope should be one-third the order, or $\zeta = p/3$. The dashed purple line indicates this prediction in Figure 4. The inertial range curves for all five temporal magnetic measurements in Figure 4(a) sit relatively near the Kolmogorov theory line but none of the lines exhibit linear behavior. This indicates that the inertial range fluctuations are multifractal and not self-similar. The spatial curves in
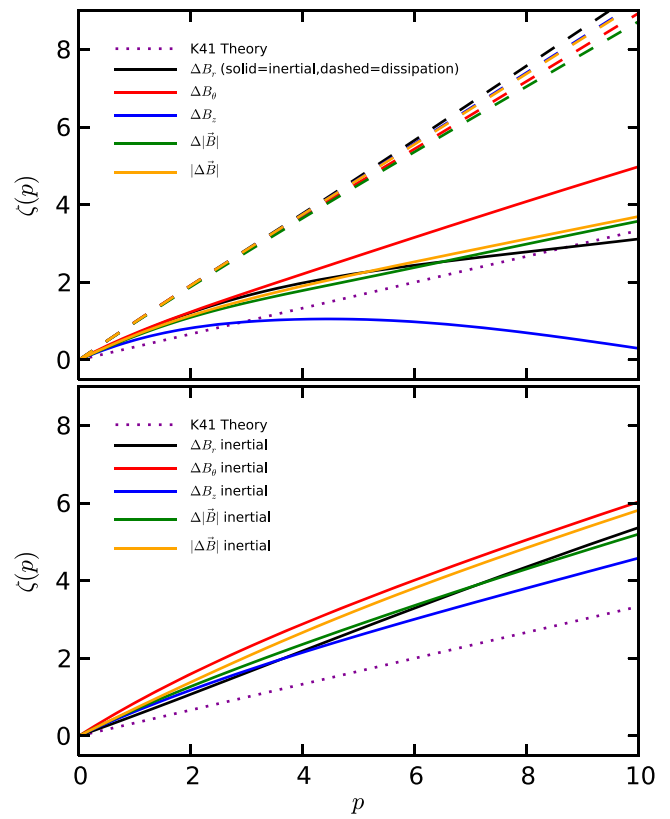

Figure 4. Scaling exponent, ζ, as a function of structure function order, p for temporal (upper) and spatial (lower) measurements. Inertial range scaling is indicated by the bold lines, while dissipation range scaling is indicated by dashed lines. Temporal scaling shows a clear distinction between multifractal (nonlinear ζ vs. p) in the inertial range and monofractal (linear ζ vs. p) in the dissipation range. The different color curves indicate the type of magnetic structure function used (i.e., B-component, B-vector magnitude, etc.)

Figure 4(b) support this observation because they are also nonlinear, though less pronounced than for the temporal data.

The dissipation range curves, in contrast, are clearly more linear. This indicates that the dissipation range fluctuations are monofractal while also having a higher level of intermittency than inertial range fluctuations. The Hurst exponents for the dissipation range are consistently about one for the various measured B values, steeper than the K41 prediction of $H = 1/3$.

6. HELICITY SCALING

The structure function analysis is also used to examine the effect of varying the amount of magnetic helicity in the plasma on the intermittency and self-similarity of the magnetic fluctuations. Previous work has shown that the degree of intermittency in fluctuations of $\dot{B} = dB/dt$ (not B), as determined by a calculation of the flatness, increases on average with an increasing amount of injected magnetic helicity (Schaffner et al. 2014c). This work revisits that result by examining the trend in B using unnormalized structure functions and the resulting relationship between structure function slope and p.

Figure 5 shows the slope versus the order for eight different helicity states for inertial range fluctuations (solid lines) and dissipation range fluctuations (dashed lines). Recalling that the steepness of the slope is indicative of a relative degree of intermittency, the order of the inertial range curves for each
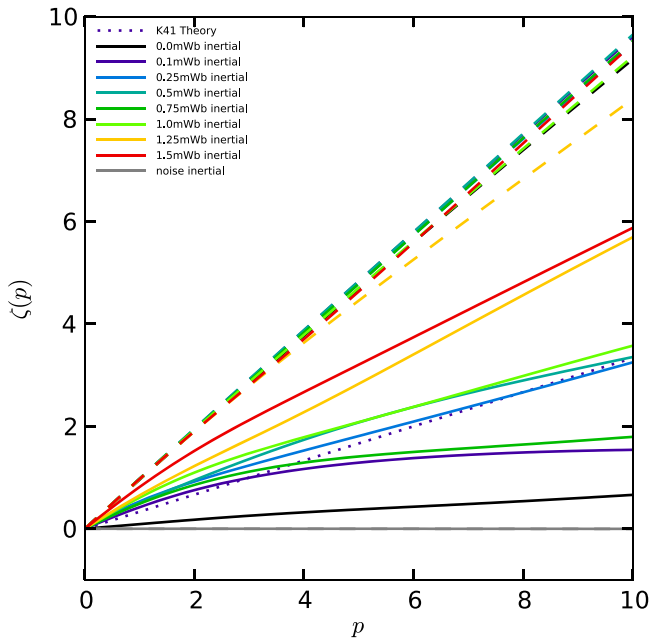
Figure 5. Scaling exponent vs. order for different values of magnetic helicity (as set by the amount of initial flux in the plasma gun; Schaffner et al. 2014c). Inertial range intermittency increases with helicity as shown by increasingly steeper curves in the inertial range. The dissipation range scaling appears to be unaffected by the change in helicity.

helicity indicates increasing intermittency with increasing helicity, which is again consistent with the findings for an analysis of $\dot{B}$ time series (Schaffner et al. 2014c). However, the structure function analysis here further shows that with the exception of the zero helicity state, the inertial range turbulence for any helicity is not self-similar. The dissipation range lines, however, show that the dissipation range intermittency is self-similar regardless of the amount of injected magnetic helicity in the plasma.

7. DISCUSSION

The observation of both multifractal and monofractal scaling of magnetic fluctuation structure functions in SSX has implications for both the dissipative nature of the turbulence and for the universality of MHD turbulence. Like that observed in Kiyani et al. (2013), the transition between multifractal scaling of the inertial range and monofractal scaling of the dissipation range is rapid. This suggests that the dissipation mechanism is independent of the scale of the turbulence structures—in other words, the dissipation scale is absolute rather than relative. This is in contrast to the predictions and observations made for hydrodynamic turbulence where viscosity is the known dissipation mechanism. In those cases, each scaling exponent has a corresponding dissipation scale due to the viscosity. As smaller and smaller scales are approached, the viscosity "shuts-off" the scaling exponents gradually producing a scaling transition region from multifractal inertial to monofractal dissipation ranges (Benzi et al. 1984; Frisch & Vergassola 1991). If the dissipation mechanism has an absolute scale, independent of each scaling exponent, then a rapid transition would be observed as this absolute scale is passed. Kiyani et al. (2010) discusses the possibility that a dissipation scale associated with the ion inertial length may be at play. However, it is often difficult to distinguish the ion gyroscale

(ρ_i) effects versus ion inertial scale (δ_i) effects in super-Alfvenic solar wind since $\beta \approx 1$. This laboratory turbulence, however, has a more resolved separation between ρ_i and δ_i (Schaffner et al. 2014a), and the results presented here show the multifractal to monofractal scaling transition occurring at around δ_i rather than ρ_i. Though evidence for the existence of current sheets has been demonstrated in previous SSX experiments on reconnection using stable spheromaks (Brown et al. 2012), more concrete evidence for the presence of current sheets in this more turbulent SSX plasma is still being sought; however, there is preliminary evidence from the helicity scan work (Schaffner et al. 2014c) that these current sheets may indeed be present. These current sheets, then, could play the role of an absolute dissipation scale. It should be noted, however, that an alternative solar wind intermittency analysis (Alexandrova et al. 2008) does not exhibit a transition in scaling from inertial to dissipation range and the authors of this work suggest the existence of a compressible inertial range cascade rather than a dissipation range.

Another interesting comparison between the results in Kiyani (2013) and those presented here is the difference in collisionality. The solar wind is a collisionless plasma with mean-free path lengths on the order of an astronomical unit (AU). The SSX plasma, while still fully ionized, is a collisional plasma with ion mean-free path lengths on the order of 0.1 cm, a bit less than one order of magnitude smaller than the ion inertial length (Schaffner et al. 2014a). While in MHD turbulence theory, resistivity can be thought to play a role for magnetic turbulence as viscosity would for velocity turbulence, the resistivity does not appear to have the same affect for dissipation given the comparison in scaling between the collisionless solar wind and the collisional laboratory plasma. This result begs the question of what role ion viscosity might have in the turbulent dissipation process as well as indicate possible universality of MHD turbulence regardless of collisionality.

8. CONCLUSIONS

This paper has presented the results of a detailed structure function analysis of turbulent magnetic fluctuations in a laboratory plasma experiment. The structure functions indicate a distinction between multifractal scaling in inertial range regimes and monofractal scaling in dissipation range regimes. Multifractal scaling is observed in both temporal fluctuations as well as spatial fluctuations. Monofractal scaling is seen only in temporal fluctuations due to the limitations of spatial measurement resolution. The work also shows that intermittency and scaling can be modified by the magnetic helicity of the turbulent plasma; increasing helicity corresponds to increased intermittency in the inertial range and modification of the scaling exponents as a function of order. However, helicity does not appear to affect the monoscaling results of the dissipation scale. These results compare favorably to a similar analysis of inertial range and dissipation range turbulence in the solar wind (Kiyani et al. 2013), which suggests some amount of universality between the two MHD systems despite differences in collisionality.

REFERENCES

Alexandrova, O., Carbone, V., Veltri, P., & Sorriso-Valvo, L. 2008, ApJ, 674, 1153

Anselmet, F., Gagne, Y., Hopfinger, E. J., & Antonia, R. A. 1984, JFM, 140, 63

Benzi, R., Paladin, G., Parisi, G., & Vulpiani, A. 1984, JPhA, 17, 3521

Biskamp, D. 1994, PhRvE, 50, 2702

Biskamp, D., & Müller, W.-C. 2000, PhPl, 7, 4889

Boldyrev, S. 2002, ApJ, 569, 841

Brown, M. R., Cothran, C. D., Gray, T., Myers, C. E., & Belova, E. V. 2012, PhPl, 19, 080704

Brown, M. R., & Schaffner, D. A. 2014, PSST, 23, 063001

Brown, M. R., & Schaffner, D. A. 2015, JPlPh, 81, 345810302

Bruno, R., & Carbone, V. 2013, LRSP, 10, 2

Burlaga, L. F. 1991, JGR, 96, 5847

Burlaga, L. F. 1992, JGR, 97, 4283

Carbone, V. 1993, PhRvL, 71, 1546

Chevillard, L., Castaing, B., & Leveque, E. 2005, EPJB, 45, 561

Cho, J., Lazarian, A., & Vishniac, E. T. 2003, ApJ, 59, 812

Consolini, G., Marcucci, M. F., & Candidi, M. 1996, PhRvL, 76, 4082

Dubrulle, B. 1994, PhRvL, 73, 959

Frisch, U. 1995, Turbulence (Cambridge: Cambridge Univ. Press)

Frisch, U., & Vergassola, M. 1991, EL, 14, 439

Hnat, B., Chapman, S. C., Rowlands, G., Watkins, N. W., & Freeman, M. P. 2003, GeoRL, 30, 2174

Kiyani, K., Chapman, S., Khotyaintsev, Y., Dunlop, M., & Sahraoui, F. 2010, in AIP Conf. Proc. 1216, Twelfth Int. Solar Wind Conf., Fractal Dissipation of Small-Scale Magnetic Fluctuations in Solar Wind Turbulence as Seen by CLUSTER, Vol. 136, ed. M. Maksimovic et al. (Melville, NY: AIP)

Kiyani, K. H., Chapman, S. C., Khotyaintsev, Yu. V., Dunlop, M. W., & Sahraoui, F. 2009, PhRvL, 103, 075006

Kiyani, K. H., Chapman, S. C., Sahraoui, F., et al. 2013, ApJ, 763, 10

Kolmogorov, A. N. 1941, DoANT, 30, 301

Kolmogorov, A. N. 1962, JFM, 13, 82

Marsch, E., & Tu, C.-Y. 1997, NPGeo, 4, 101

Meneveau, C., & Sreenivasan, K. R. 1987, PhRvL, 59, 1424

Müller, W.-C., & Biskamp, D. 2000, PhRvL, 84, 475

Osman, K. T., Matthaeus, W. H., Gosling, J. T., et al. 2014, PhRvL, 112, 215002

Pagel, C., & Balogh, A. 2002, JGR, 107, SSH 6-1

Paladin, G., & Vulpiani, A. 1987, PhR, 156, 147

Schaffner, D. A., Brown, M. R., & Lukin, V. S. 2014a, ApJ, 790, 126

Schaffner, D. A., Lukin, V. S., Wan, A., & Brown, M. R. 2014b, PPCF, 56, 064003

Schaffner, D. A., Wan, A., & Brown, M. R. 2014c, PhRvL, 112, 165001

She, Z.-S., & Leveque, E. 1994, PhRvL, 72, 336

Tu, C.-Y., & Marsch, E. 1995, SSRv, 73, 1